ISSN 1070-3284, Russian Journal of Coordination Chemistry, 2019, Vol. 45, No. 10, pp. 741–747. © Pleiades Publishing, Ltd., 2019.

Novel Zn and Cd Coordination Polymers Assembled from Imidazole-Based Zwitterionic Ligands: Synthesis, Crystal Structures, and Luminescence Properties

P. Yang[a], G. Xiong[a, *], Y. K. He[a], L. X. You[a], B. Y. Ren[a], and Y. G. Sun[a, **]

[a] *The Key Laboratory of Inorganic Molecule-Based Chemistry of Liaoning Province, Shenyang University of Chemical Technology, Shenyang, 110142 P.R. China*

**e-mail: xg@syuct.edu.cn*

***e-mail: sunyaguang@syuct.edu.cn*

Received May 30, 2018; revised October 14, 2018; accepted November 24, 2018

Abstract—Two transition-metal coordination polymers $\{[Zn_2(L)_2(HCOO)_2]\}_n$ (**I**) and $\{[Cd_2(L)_3(HCOO)] \cdot 2H_2O\}_n$(**II**) (L = 1,3-bis(4-(methoxycarbonyl)benzyl)-1*H*-imidazol-3-ium anion) have been synthesized via solvo-thermal method. Both of the coordination polymers **I** and **II** were characterized by single-crystal X-ray diffraction (CIF files CCDC nos. 1834629 (**I**) and 1834630 (**II**)), FT-IR spectroscopy, elemental analysis and thermogravimetric analysis. The results shown compound **I** is a two dimensional **sql** layer structure containing interlocking structure between the left and right helix chains, and compound **II** is rare three dimensional six-fold interpenetrating **dia** topology framework. Luminescence investigations revealed that both of compound **I** and **II** emitted blue light.

Keywords: coordination polymers, zwitterionic ligands, luminescence

DOI: 10.1134/S1070328419100087

INTRODUCTION

The purpose of synthetic different coordination polymers is to pursue new function materials originating from metal centers, ligands and the space constructed by metal centers and ligands. Therefore, the design of ligands is particularly important for the construction and modification of coordination polymers [1–5]. An interesting ligand not only endows the coordination polymer with novel functions, but also brings plentiful post-modification reactions on ligand for bringing more novel and interesting functions [6, 7]. For example, NH_2-substituted ligands were used to construct coordination polymers due to the Lewis base sites are easily modified by aldehydes, anhydride and so on [8–10]. However, in fact, the organic functional groups that can be modified in coordination polymers are relatively rare.

Imidazole-based zwitterionic ligands can be used as precursors of N-heterocyclic (NHC) ligands, and their complexes exhibit potential applications as green clean catalysts and luminescent materials [11]. Therefore, imidazole-based zwitterionic ligands are purposefully introduced into coordination polymers, making them as the precursors of NHC ligands, which can coordinate with various metal ions via post-modification [12]. While, the number of coordination polymers constructed by imidazolium-based zwitterionic ligands is much smaller than that of coordination polymers assembled by other ligands. Here, we have designed flexible imidazolium-based zwitterionic ligand (L = 1,3-bis(4-(methoxycarbonyl)benzyl)-1*H*-imidazol-3-ium anion) to synthesize two novel coordination polymers $\{[Zn_2(L)_2(HCOO)_2]\}_n$ (**I**) and $\{[Cd_2(L)_3(HCOO)] \cdot 2H_2O\}_n$ (**II**) under solvothermal conditions, respectively. Compound **I** is a two dimensional **sql** layer structure containing interlocking structure between the left and right helix chains, and compound **II** is rare three dimensional six-fold interpenetrating **dia** framework. Both of compound **I** and **II** emitted blue light via luminescence investigations.

EXPERIMENTAL

Materials and methods. All chemicals purchased were of reagent grade and used without further purification. ^{1}H NMR spectra were recorded on a JEOL JNM-LA500FT instrument (500 MHz) in $CDCl_3$ with TMS as the internal standard. The elemental analyses (C, H, and N) were carried out applying a Perkin-Elmer 240C elemental analyzer. The IR spectra in the 4000–400 cm^{-1} region were measured using a Nicolet IR-408 spectrometer and KBr pellets. Powder X-ray diffraction (PXRD) data were collected using a BRUKER D8 ADVANCE diffractometer

using CuK_α (λ = 1.542 Å). Thermogravimetric (TG) curve was recorded from room temperature to 800°C with the heating rate of 10°C/min on a Netzsch TG 209 instrument undernitrogen atmosphere. The Solid fluorescence emission and excitation spectra were measured on a Horiba Scientific fluorescence.

Synthesis of ester of H_2L. Imidazole (0.136 g, 2.00 mmol) and K_2CO_3 (0.415 g, 3.00 mmol) were stirred for 15 min in 100 mL of MeCN. Then methyl 4-(bromomethyl)benzoate (0.916 g, 4.00 mmol) was added subsequently and stirred for 5 days. And then the mixture was filtered, and the MeCN in resulting solution was removed via the reduced pressure distillation. Finally, 150 mL H_2O was added, then stirred the mixture for 30 min. The white solid was filtered, washed with Et_2O (3 × 20 mL), and dried in suction [13]. White crystalline powder was obtained (0.219 g, 0.6 mmol, 30%).

IR (KBr; ν, cm^{-1}): 3145 w., 3085 m., 3041 m., 2976 m., 1719 v.s., 1614 m., 1550 m., 1437 m., 1289 v.s., 1188 s., 1151 s., 1107 s., 1023 m., 963 m., 873 s., 803 m., 737 s., 652 m., 618 m. ^{1}H NMR (500 MHz; $CDCl_3$, δ, ppm): 11.22 (s., NCHN); 8.09 (d., J = 8.0, $4H_{ar}$); 7.56 (s., 2CH=); 7.12 (d., J = 8.0, $4H_{ar}$); 5.68 (s., $2CH_2$); 3.94 (s., 2 MeO).

The synthesis routine of ester H_2L is given below:

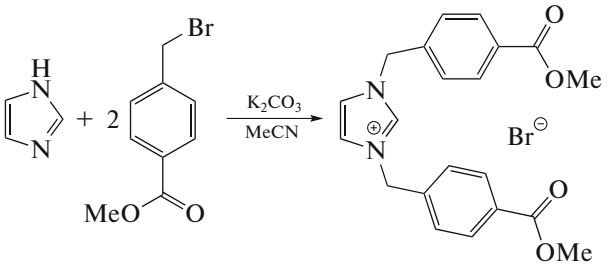

Synthesis of I. Ester of H_2L (9.1 mg, 0.025 mmol) and $Zn(NO_3)_2 \cdot 6H_2O$ (11 mg, 0.039 mmol) were thoroughly dissolved in a mixed solvent of 2 mL water and 10 mL DMF and heated to 120°C for 96 h in a 23 mL Teflon-lined stainless-steel autoclave and then cooled to room temperature at a rate of 5°C/h. Colorless cubic crystal particles were obtained after several days. The yield was 90% (based on H_2L).

For $C_{40}H_{32}N_4O_{12}Zn_2$

Anal. calcd., %	C, 53.84	H, 3.58	N, 6.28
Found, %	C, 53.70	H, 3.45	N, 6.17

IR (KBr; ν, cm^{-1}): 3093 w., 3042 w., 1616 v.s., 1557 m., 1374 v.s., 1154 s., 747 s., 623 m.

Synthesis of II. The mixture of ester of H_2L (9.4 mg, 0.026 mmol) and $Cd(NO_3) \cdot 6H_2O$ (11 mg, 0.039 mmol), 5 mL H_2O and 5 mL DMF was heated to 100°C for 96 h in a 20 mL glass vial, and then cooled to room temperature, finally colorless needle crystals were afforded. The crystalline solid of **II** can be obtained in a range temperature from 85 to 160°C. The different reaction conditions are responsible for the sizes of the needle-shaped crystals. The yield was 80% (based on H_2L).

For $C_{29}H_{25}N_3O_8Cd$

Anal. calcd., %	C, 53.05	H, 3.81	N, 6.40
Found, %	C, 52.90	H, 3.675	N, 6.36

IR (KBr; ν, cm^{-1}): 3123 m., 3094 m., 1597 v.s., 1544 v.s., 1398 v.s., 1513 s., 859 s., 747 s., 624 s.

X-ray crystallography. Diffraction data for complex **I** and **II** were recordedon a Bruker SMART Apex CCD diffractometer using graphite-monochromat MoK_α radiation (0.71073 Å) at 293 K in the ω–2θ scan mode. The single crystal data of **II** was mounted on an Oxford diffractometer Super Nova TM at 120(2) K with a graphite-monochromatic MoK_α radiation (λ = 0.71073 Å) using the ω–scan technique. Using Olex2 [14], the structure was solved by the ShelXS structure solution program and refined with the ShelXL refinement package using Least Squares minimization [15]. For **II**, the residual electron density maxima of about 5.6 e $Å^{-3}$ around the Cd(II) with the distance of 0.85 Å can be accounted for series termination errors. Hydrogen atoms were riding on carbon atoms geometrically. The crystallographic data for X-ray diffraction analysis are listed in Table 1.

Supplementary material for structures has been deposited with the Cambridge Crystallographic Data Centre (CCDC nos. 1834629 (**I**) and 1834630 (**II**); deposit@ccdc.cam.ac.uk or http://www.ccdc.cam.ac.uk).

RESULTS AND DISCUSSION

Single crystal X-ray diffraction analysis revealed that the asymmetric unit of **I** was composed of two crystallographic independence Zn atoms, two zwitterionic ligands and two formic anions which come from the decompose of DMF molecules (Fig. 1a). The Zn(1) atom is five-coordinate with two oxygen atoms (O(2), O(3)) from one bidentate chelation carboxylate group of zwitterionic ligands, two oxygen atoms (O(4), O(5)) of two formic anions, and one oxygen atom (O(1)) from one monodentate carboxylate group of zwitterionic ligand. The Zn(2) atom was located in the center of tetrahedron constructed by two oxygen atoms (O(7), O(8)) from two monodentate carboxylate groups of two zwitterionic ligands and two oxygen atoms (O(4), O(6)) from two formic anions. The Zn–O bond distances ranged from 1.950 to 2.487 Å. Two carboxyl groups of zwitterionic ligands employed the monodentate mode to link adjacent Zn(1) cations to form right-helix chain, while adjacent Zn(2) cations were linked by the mean of bidentate chelation of carboxyl groups on zwitterionic ligands to form left-helix

Table 1. Crystallographic data and structure refinement for complexes **I** and **II**

Parameters	Value	
	I	**II**
Formula weight	891.48	655.92
Crystal system	Monoclinic	Monoclinic
Space group	$P2_1/c$	$C2/c$
a, Å	14.048(8)	24.8141(6)
b, Å	14.900(9)	11.0351(2)
c, Å	18.041(10)	19.5304(6)
β, deg	90.236(7)	98.437(3)
V, Å^3	3776(4)	5290.0(2)
Z	4	8
ρ_{calcd}, g/cm^3	1.568	1.647
μ, mm^{-1}	1.342	0.884
F(000)	1824.0	2656.0
θ Range for data collection, deg	6.032–50.012	6.198–50.018
Index ranges	$-16 \le h \le 16$, $-17 \le k \le 17$, $-21 \le l \le 21$	$-29 \le h \le 27$, $-12 \le k \le 13$, $-13 \le l \le 23$
Reflections collected	29266	9523
Independent reflections (R_{int})	6657 (0.0899), $R_{sigma} = 0.0763$	4600 (0.0213), $R_{sigma} = 0.0348$
Data/restraints/parameters	6657/0/523	4600/6/374
Goodness-of-fit on F^2	1.106	1.039
Final R indexes ($I > 2\sigma(I)$)*	$R_1 = 0.0656$, $wR_2 = 0.1146$	$R_1 = 0.0560$ $wR_2 = 0.1350$
Final R indexes (all data)*	$R_1 = 0.1062$ $wR_2 = 0.1324$	$R_1 = 0.0633$ $wR_2 = 0.1413$
Largest diff. peak and hole, e Å^{-3}	0.509 and –0.318	5.671 and –1.361

* $R_1 = \Sigma(F_o - F_c)/\Sigma(F_o)$, $wR_2 = \{\Sigma[w(F_o - F_c)^2]/\Sigma(F_o - F_c)^2\}^{1/2}$.

chain. The left and right helix chain exhibited the same pitch of 14.90 Å. The zwitterionic ligands on the left and right chain presented "U"-type geometry, which can bring out interlocking structure between the adjacent left and right helix chains (Fig. 2a). Further, the adjacent Zn(1) and Zn(2) with distance of 3.480 Å on the adjacent helix chains were linked to two dimensional structure in the *ab* plane by two type of coordination mode $^1\eta$, $^1\eta$:μ_2 and $^2\eta$:μ_2 of formic anions. From the pure topological point of view, each Zn(1)–Zn(2) unit bonded by formic anions coordinated with four zwitterionic ligands, so the Zn dimeric unit and the ligands are simplified as 4-connected nodes and lines, respectively, the framework can be simplified as a two dimensional 4-connected **sql**-type layer structure (Fig. 2b).

Single crystal X-ray diffraction analysis revealed that in the asymmetry unit, there are one Cd cation, one and half zwitterionic ligands, and half formic anion originated form decompose of DMF molecule. Each Cd cation is surrounded by seven oxygen atoms consisted by carboxyl atoms (O(1), O(2), O(3), O(4) O(5), O(6)) from three carboxyl groups of zwitterionic ligand and formate oxygen atom (O(7)) (Fig. 1b). The Cd–O bond distance were from 2.267 to 2.438 Å, which are located in reasonable range in reported coordination compounds. All of carboxyl groups employed the bidentate chelation mode to coordinate with Cd centers, while the formic anion employed the 1,3-bridged mode to link with Cd nodes. Therefore, the Cd cations can be considered as 4-connected centers. Due to the ligands coordinated with Cd cations extend along the vertex of the tetrahedron rather than the plane, so three dimensional framework is formed (Fig. 3a). After analyzing the topology, this framework can be described as a uniform 4-connected **dia** net with the point symbol of 6^6 (Fig. 3c). There are very large potential voids in single **dia** framework, which

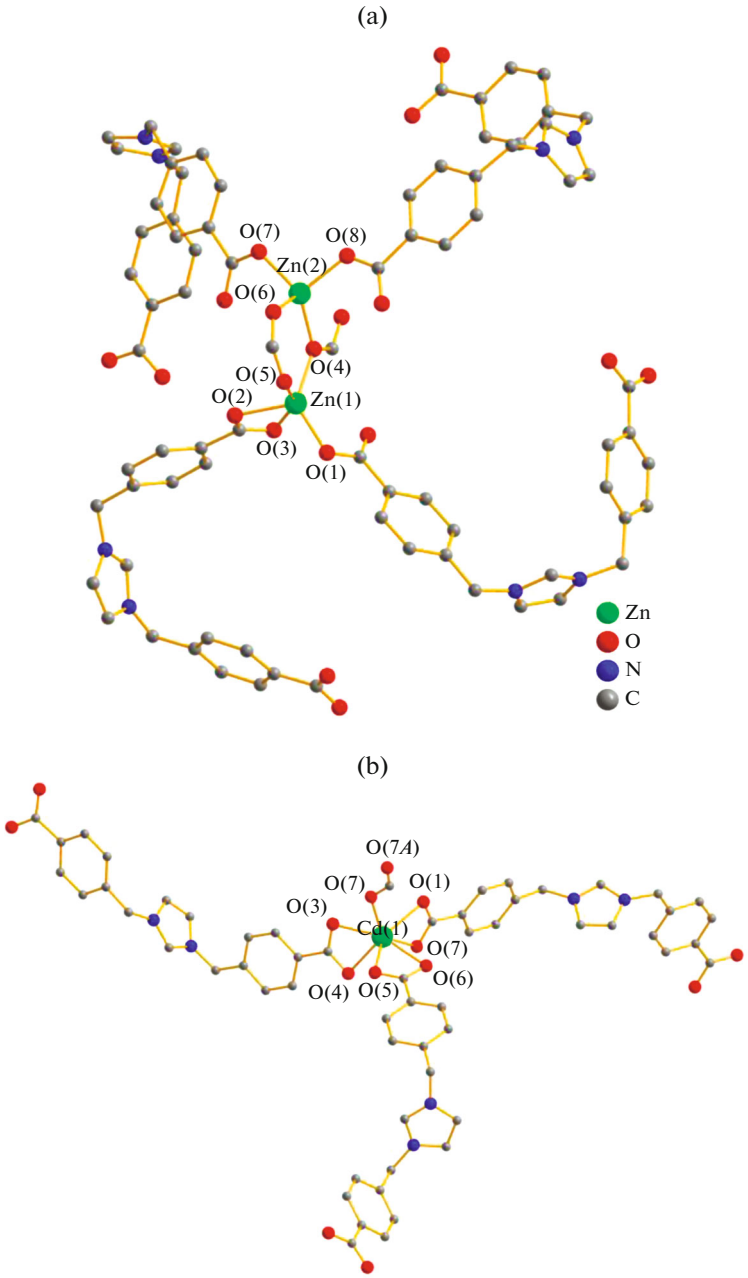

Fig. 1. The coordination environments of Zn^{2+} ion in **I** (a) and Cd^{2+} ion in **II** (b).

can lead to the poor structural steady [16]. Therefore, mutual interpenetration of six independent equivalent frameworks generate a six-fold interpenetrating and close packing architecture for increasing the structural steady (Figs. 3b and 3d). In fact, **dia**-type interpenetration structures are very common in the reported interpenetrating frameworks, but the interpenetrating numbers are mainly concentrate between 2 and 5, the six-fold interpenetrating **dia**-type framework is scarce [17–20].

To investigate the purities of compounds **I** and **II** PXRD measurements at room temperature were studied. The results revealed that the PXRD patterns obtained from experiment measurements for **I** and **II** was in good agreement with the corresponding simulated pattern from the single-crystal diffraction data, respectively, indicating a good purity and homogeneity of the sample **I** and **II**.

The TG curves of I and **II** were presented in Fig. 4. TG of **I** shows almost no weight loss before the temperature of 380°C, and above that the structure began to decompose. For **II**, 2.72% weight loss happened before 210°C was in agreement with the corresponding calculated values of 2.75% due to the loss of one lattice

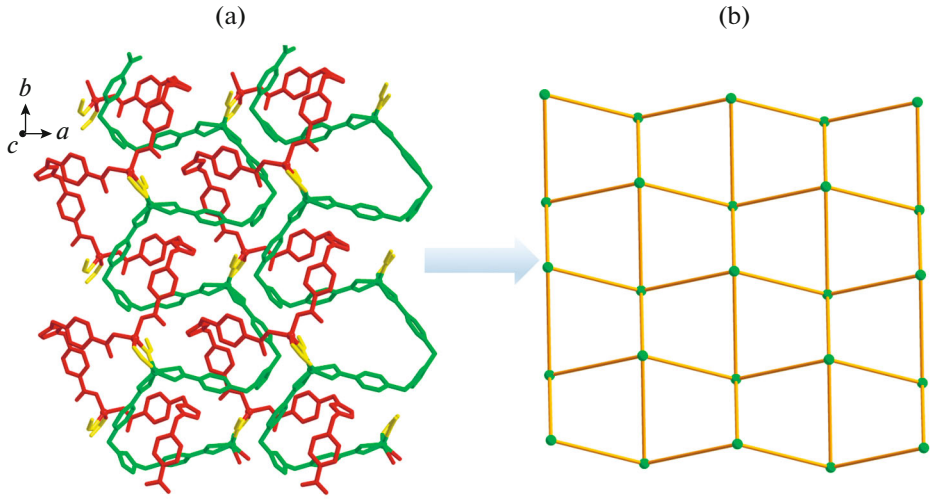

Fig. 2. The two dimensional framework of **I** in the *ab* plane (a); topological diagram of **sql** layer structure (b).

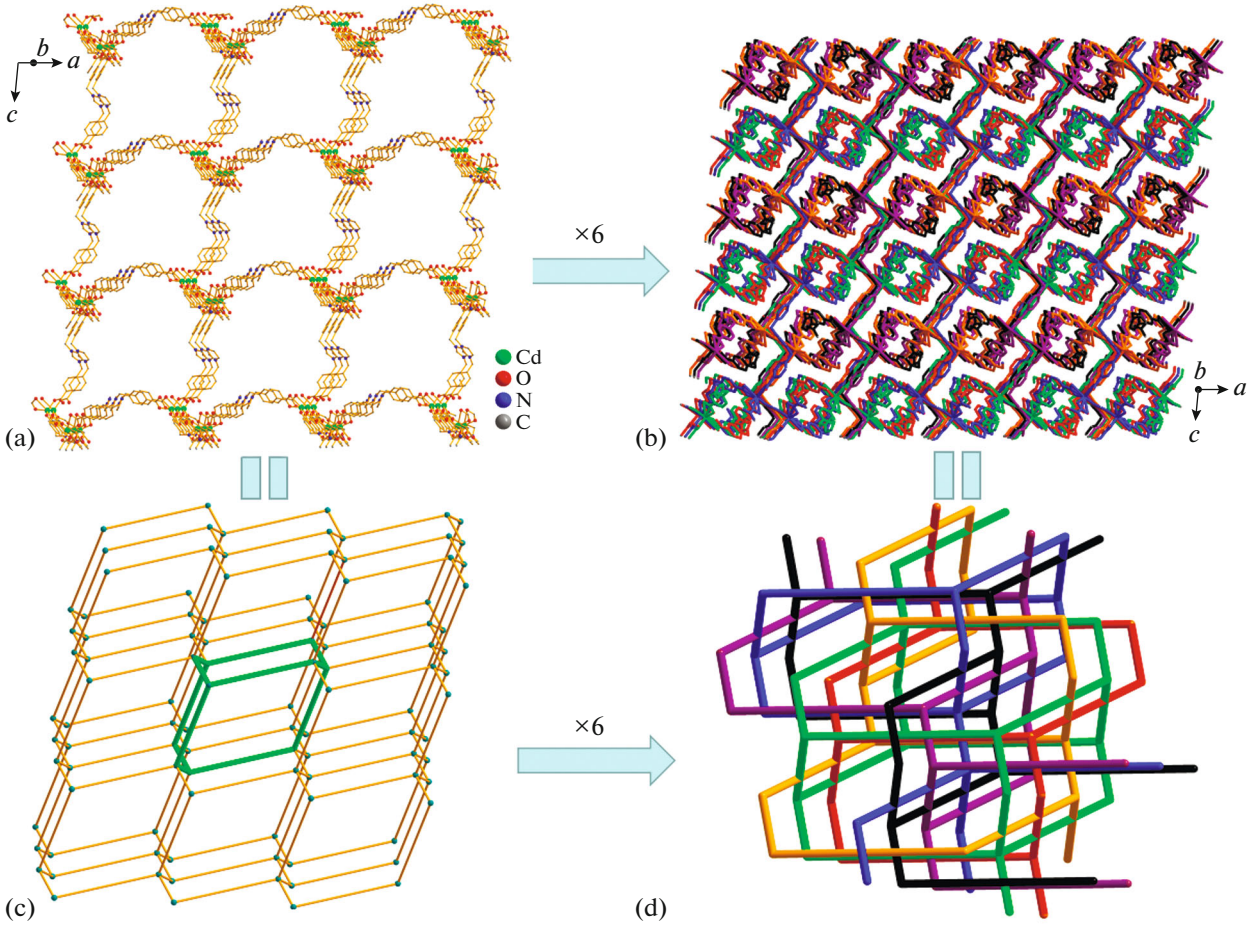

Fig. 3. View of a single **dia** framework (a); view of the six-fold interpenetrating **dia** framework (b); topological diagram of a single 3D diamond framework (c); topological diagram six-fold interpenetrating **dia** framework (d).

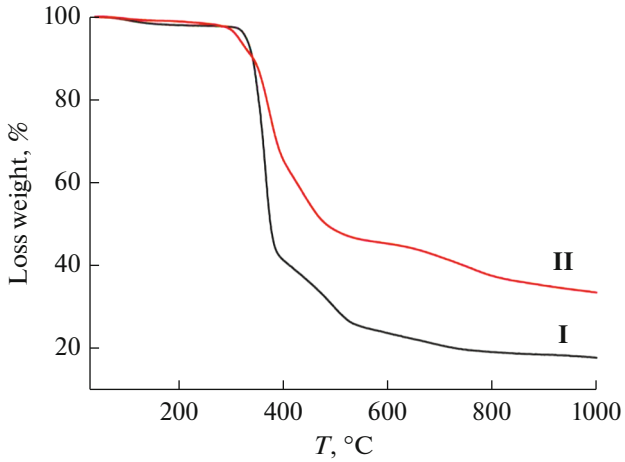

Fig. 4. TG curves of **I** and **II**.

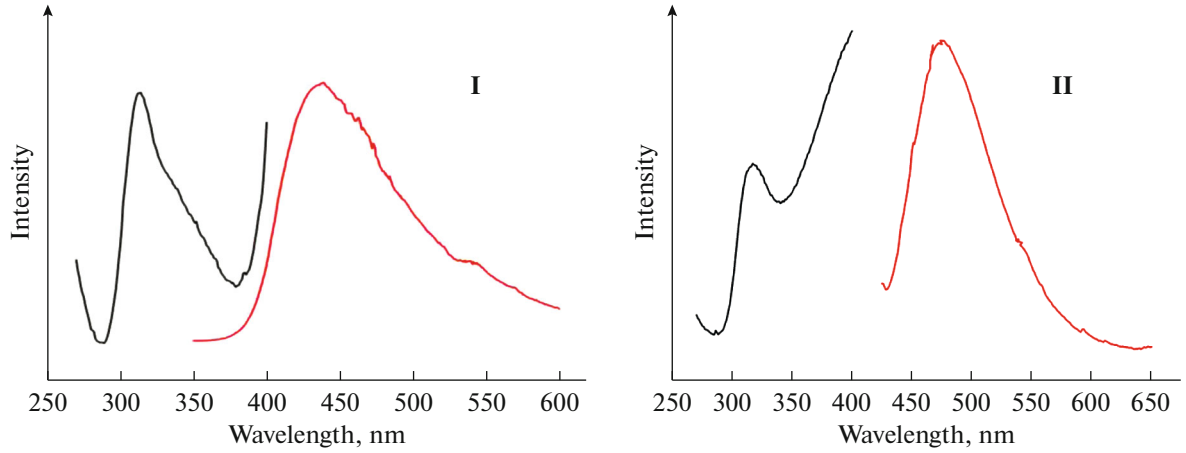

Fig. 5. The emission (red line) and excitation (black line) luminescent spectra of **I** and **II** in the solid state at room temperature.

water molecule. The frameworks of **II** was stable up to about 320°C. Thus, both of compounds **I** and **II** exhibited good thermal steady.

The luminescent properties of **I** and **II** were investigated in the solid state at room temperature (Fig. 5). The maximum adsorption peak occurred at 315 and 320 nm for **I** and **II**, respectively, which can be attributed to the $\pi \rightarrow \pi^*$ transition of ligands [21]. For **I**, the maximum emission peak occurred at 440 nm upon excitation at 315 nm, **II** exhibited maximum emission at 475 nm excited by 320 nm. Both of **I** and **II** emitted blue light which may be mainly originated from ligand–metal charge transition (LMCT) of ligands [22].

In conclusion, two Zn(II) and Cd(II) coordination polymers have been successfully assembled from flexible imidazole-based zwitterionic ligands under solvothermal conditions in this work. The results present an intriguing **sql** layer structure for **I** containing interlocking structure between the adjacent left and right helix chains and **dia** topology with rare six-fold interpenetrating nets for **II**. Moreover, structure stabilities and luminescent were also investigated. This work will further enrich the synthesis of imidazolezwitterionic ligands-based coordination polymers, which can be used as the precursors of NHC ligands to build novel NHC catalysts and luminescent materials.

ACKNOWLEDGMENTS

This work was supported by the Natural Science Foundation of China (nos. 21671139 and 21501122), the Distinguished Professor Project of Liaoning province (2013204) and Doctoral Scientific Research Foundation of Liaoning Province (201601193 and 201601201).

REFERENCES

1. Stock, N. and Biswas, S., *Chem. Rev.*, 2012, vol. 112, p. 933.

2. Chen, Y., Wang, D.K., Deng, X.Y., et al., *Catal. Sci. Technol.*, 2017, vol. 7, p. 4893.
3. Wang, K., Xia, B., Wang, Q.L., et al., *Dalton Trans.*, 2017, vol. 46, p. 1042.
4. Suresh, P., Babu, C.N., Sampath, N., et al., *Dalton Trans.*, 2015, vol. 44, p. 7338.
5. Sun, Y.N., Xiong, G., Ding, F., et al., *Inorg. Chem. Commun.*, 2015, vol. 62, p. 103.
6. Timur, I., Subhadip, G., Li, Z.Y., et al., *Acc. Chem. Res.*, 2017, vol. 50, p. 805.
7. Karmakar, A., Paul, A., Rubio, G.M.D.M., et al., *Eur. J. Inorg. Chem.*, 2016, vol. 36, p. 5557.
8. Kim, A. and Seong, H., *CrystEngComm*, 2016, vol. 18, p. 3524.
9. Li, L.J., Tang, S.F., Wang, C., et al., *Chem. Commun.*, 2014, vol. 50, p. 2304.
10. Robinson, W., Flaig, T.M., Osborn, P., et al., *J. Am. Chem. Soc.*, 2017, vol. 139, p. 12125.
11. Paladugu, S., Soumya, R., Chatla, N.B., et al., *Dalton Trans.*, 2013, vol. 42, p. 10838.
12. Chizoba, I., Ezugwuab, N., Alam, K., and Mekhman, Y.F., *Coord. Chem. Rev.*, 2015, vol. 307, p. 188.
13. Siddappa, P., Karolin, D., Anthony, D., et al., *Helv. Chim. Acta*, 2010, vol. 93, p. 2347.
14. Dolomanov, O.V., Bourhis, L.J., Gildea, R.J., et al., *J. Appl. Cryst.*, 2009, vol. 42, p. 339.
15. Sheldrick, G.M., *SHELXS-97, Program for Crystal Structure Determination,* Göttingen: Univ. of Göttingen, 1997.
16. Lee, H.J., Kwon, H., Sim, J., et al., *CrystEngComm*, 2017, vol. 19, p. 1528.
17. Tan, Y.X., Si, Y.N., Wang, W.J., and Yuan, D.Q., *J. Mater. Chem., A*, 2017, vol. 5, p. 23276.
18. Pickwick, B.L., Pochodylo, A.L., and LaDuca, R.L., *Inorg. Chim. Acta*, 2017, vol. 466, p. 618.
19. Zhang, Y., Wang, L., and Zeng, M.H., *Inorg. Chem. Commun.*, 2017, vol. 83, p. 123.
20. Shi, Z.Z., Qing, L., and Zheng, H.G., *Dalton Trans.*, 2017, vol. 46, p. 4589.
21. Vasylevskyi, S.I., Regeta, K., Ruggi, A., et al., *Dalton Trans.*, 2018, vol. 47, p. 596.
22. Jia, L.M., Tong, J., and Yu, S.Y., *J. Photochem. Photobiol., A.*, 2018, vol. 355, p. 84.